Modulation of mTOR signaling by radiation and rapamycin treatment in canine mast cell cancer cells

Morla Phan, Changseok Kim, Anthony Mutsaers, Valerie Poirier, Brenda Coomber

Abstract

Rapamycin has been reported to reduce cancer cell survival in certain tumors following radiation therapy, but the mechanisms driving this phenomenon are unclear. Rapamycin inhibits mTOR signaling, a pathway responsible for several essential cell functions. The objective of this study was to investigate the effects of rapamycin and radiation on the activation and inhibition of mTOR signaling and the relationship between mTOR signaling and DNA damage response *in vitro* using canine mast cell tumor (MCT) cancer cell lines. Rapamycin rapidly inhibited S6K phosphorylation in a dose-dependent manner. Ionizing radiation (3, 6, or 10 Gy) was able to activate mTOR signalling, but the combination of radiation and rapamycin maintained mTOR inhibition. The comet assay revealed that co-treatment with rapamycin induced modest increases in the severity of DNA damage to MCT cells, but that these differences were not statistically significant. Although the relationship between mTOR and DNA damage response in MCT cancer cell lines remains unclear, our findings suggest the possibility of interaction, leading to enhancement of radiation response.

Résumé

Il a été rapporté que la rapamycine réduisait la survie des cellules cancéreuses dans certaines tumeurs après une radiothérapie, mais les mécanismes à l'origine de ce phénomène ne sont pas clairs. La rapamycine inhibe la signalisation mTOR, une voie responsable de plusieurs fonctions cellulaires essentielles. L'objectif de cette étude était d'étudier les effets de la rapamycine et des radiations sur l'activation et l'inhibition de la signalisation mTOR et la relation entre la signalisation mTOR et la réponse aux dommages à l'ADN in vitro *à l'aide de lignées cellulaires cancéreuses de tumeurs mastocytaires canines (MCT). La rapamycine a rapidement inhibé la phosphorylation de S6K de manière dose-dépendante. Le rayonnement ionisant (3, 6 ou 10 Gy) a pu activer la signalisation mTOR, mais la combinaison de rayonnement et de rapamycine a maintenu l'inhibition de mTOR. Le test des comètes a révélé que le co-traitement avec la rapamycine induisait des augmentations modestes de la gravité des dommages à l'ADN des cellules MCT, mais que ces différences n'étaient pas statistiquement significatives. Bien que la relation entre mTOR et la réponse aux dommages à l'ADN dans les lignées cellulaires cancéreuses MCT reste incertaine, nos résultats suggèrent la possibilité d'une interaction, conduisant à une amélioration de la réponse aux radiations.*

(Traduit par Docteur Serge Messier)

Introduction

Dogs commonly develop malignancies of mast cells in the form of solid mast cell tumors (MCTs), most often located in the dermis or subcutaneous tissue (1). Genetics is suspected to play a strong role in MCT development, demonstrated by the risk disparity among breeds and the presence of a c-KIT mutation that causes constitutive activation in approximately 25% of cases (2,3).

Surgery is the primary method of treatment for these tumors. Although surgery alone is typically sufficient to control low-grade tumors, high-grade tumors have an increased risk of local recurrence and metastasis (4). Surgery can be combined with an adjuvant therapy, such as radiation for local control or with chemotherapy or tyrosine kinase inhibitors for systemic control (5,6). Combination treatment reduces risks associated with local recurrence and metastasis, especially in high-grade tumors.

Radiation therapy (RT) alone is mainly palliative (7), demonstrating the most curative potential as an adjuvant to surgery or chemotherapy (8). When cancer cells develop mechanisms, such as increasing DNA damage response (DDR), in order to resist the consequences of DNA damage caused by ionizing radiation, the effectiveness of RT is reduced (9,10).

Several studies *in vitro* reported that the effectiveness of RT can be enhanced in different cancers such as lung and cervical by using rapamycin (RAPA) or its derivatives to block mTOR signaling, a nutrient-sensing pathway central to several essential cell functions, such as growth, proliferation, and survival (11–13). Environmental cues, such as growth factors or nutrients, can activate mTOR, which

Department of Biomedical Sciences (Phan, Mutsaers, Coomber) and Department of Clinical Studies (Kim, Mutsaers, Poirier), Ontario Veterinary College, University of Guelph, Guelph, Ontario N1G 2W1.

Address all correspondence to Dr. Brenda Coomber; telephone: 1-519-824-4120, ext. 54922; email: bcoomber@uoguelph.ca

Received May 16, 2021. Accepted July 18, 2021.

results in the formation of protein complex mTORC1 (14). mTORC1 then phosphorylates p70S6K, which has become a standard marker for assessing mTOR activation (15).

We were interested in understanding the intersection of the highly conserved mTOR signaling and DDR in canine mast cell tumors. The objective of this study was, therefore, to examine the effects of RAPA and radiation on the activation and inhibition of mTOR signaling and their effects on DNA damage *in vitro* using cell lines generated from spontaneously occurring canine mast cell tumors.

Materials and methods

Cell culture

Two canine mast cell cancer cell lines, MCT-1 and MCT-2, were previously developed and characterized by our laboratory (16). They were maintained in RPMI 1640 (Sigma Aldrich, Oakville, Ontario), supplemented with 10% fetal bovine serum (FBS) (Gibco/ThermoFisher Scientific, Waltham, Massachusetts, USA) and 1% Penicillin/Streptomycin (HyClone Laboratories, Logan, Utah, USA) at 37°C and 5% carbon dioxide (CO_2). Cells grew to about 80% confluency in 100-mm dishes for each experiment. Confluency of adherent MCT-1 cells was determined through visual inspection, whereas confluency for the suspension MCT-2 cells was determined by the color of the pH indicator in the media and visual inspection.

Treatment conditions

A total of 250 000 cells were seeded into 6-well plates and allowed to grow to 80% confluency. Rapamycin (RAPA) was purchased from Cell Signaling Technologies (Danvers, Massachusetts, USA) and dissolved in dimethyl sulfoxide (DMSO) to a stock concentration of 10 mM, which was then stored at −80°C. This stock solution was diluted in media to concentrations of 5.5, 11, or 16.5 nM, which correspond to 50%, 100%, and 150% of the plasma steady-state doses previously reported in dogs (17). Rapamycin was diluted immediately before being added to MCT cells. The vehicle control was a volume of DMSO equivalent to 11 nM or 16.5 nM of RAPA for the comet assay and 16.5 nM of RAPA only for western blotting.

Radiation doses of 3, 6, or 10 Gy were administered to cells using a Varian Clinac iX linear accelerator (Varian, Palo Alto, California, USA). These doses were chosen for their relevance to current veterinary clinical practices (18–20). The dose distribution of the experimental setup has been verified by a medical physicist and described in a previous study (21). Control plates were removed from the incubator and transported to and from the radiation center along with experimental plates but received 0 Gy of radiation.

Clonogenic survival assay

MCT-1 cells were grown to ~80% confluence, then pre-treated in RPMI 1640 supplemented with 10% FBS with vehicle control (DMSO); 5.5 nM RAPA; 11 nM RAPA; or 16.5 nM RAPA. The vehicle control was incubated for 48 h, whereas the RAPA pre-treatment groups were incubated for 24 or 48 h. Each treatment group was then trypsinized and the cells were pelleted and redistributed into 6-well plates. Plates for either 3 or 6 Gy IR had duplicate wells with 100, 1000, or 10 000 cells/well; plates set to receive 10 Gy IR had duplicate wells with 100, 1000, or 20 000 cells/well.

After 24 h, plates were placed between 2 solid water equivalent plates with thicknesses of 4.5 cm and 5 cm for the top and bottom plates, respectively. Each pre-treatment group was given a dose of 0 Gy, 3 Gy, 6 Gy, or 10 Gy; the dose distribution was verified by a medical physicist. The 0 Gy plates were brought to the radiation facility but were not irradiated. After irradiation, all plates were incubated at 37°C and 5% CO_2 for 2 wk, then cells were stained with Crystal Violet. Colonies with > 50 cells or more were counted to assess cell survival. The vehicle control 0 Gy treatment group was used as the reference point and clonogenic survival was calculated as:

$$\left\{\frac{\left(\frac{\text{Number of colonies formed in Treatment Group}}{\text{Number of cells seeded in Treatment Group}}\right)}{\left(\frac{\text{Number of colonies formed in DMSO Control}}{\text{Number of cells seeded in DMSO Control}}\right)}\right\} \times 100$$

Western blotting

Cells were seeded in 6-well plates and treated with 5.5, 11, or 16.5 nM of RAPA alone; 3, 6, or 10 Gy of radiation alone; or a combination. For the combination treatment, the media was replaced with media containing the appropriate concentration of RAPA immediately before radiation. At the time points of interest, whole-cell protein lysates were obtained using Cell Lysis Buffer (Cell Signaling Technologies) with aprotinine, Protease Inhibitor Cocktail II, and phenylmethylsulfonyl fluoride (Sigma Life Science, St. Louis, Missouri, USA). Next, 100 μL of sodium orthovanadate solution (33.25 μL of PBS, 12.5 μL of 100 mM sodium orthovanadate, and 2.5 μL of 3% hydrogen peroxide per milliliter of media) was added to each well 15 min before lysing.

For the 1-minute timepoint for MCT-1 cells, sodium orthovanadate was added to the media for 15 min, after which the media was aspirated and RAPA-treated media was added and then removed to begin the lysing process, which took about 60 s. For the 4-minute timepoint for MCT-2 cells, cells were transferred to a 15-mL tube and sodium orthovanadate was added to the media for 15 min. Rapamycin was then added and the tube was inverted, then immediately centrifuged to pellet the cells. The media was aspirated and the pellet was washed with PBS, re-pelleted, and then lysed.

Lysates were stored at −80°C in 10-μL aliquots. Protein concentrations were quantified using the Bio-Rad protein assay. Samples containing 25 μg of protein were electrophoresed through 10% polyacrylamide gels. Proteins were transferred onto polyvinylidene fluoride (PVDF) membranes and stained with Amido black to confirm a successful transfer. Membranes to be probed for phospho-ribosomal protein S6 kinase (S6K) were blocked with 5% bis(trimethylsilyl)acetamide (BSA) for 1 h at room temperature. Membranes to be probed for native S6K and tubulin were blocked with 5% skim milk for 1 h at room temperature. Membranes were incubated overnight at 4°C while being gently rocked, with the primary antibody diluted with the same blocking solution in a 1:1000 ratio.

The secondary antibody was diluted with 5% skim milk in a 1:10 000 ratio. A BioRad ChemiDoc XRS+ and Immobilon Forte (Millipore Sigma, Burlington, Massachusetts, USA) was used to

image chemiluminescence. Monoclonal antibodies for both the phosphorylated (Thr389) (catalog #9234) and native forms of S6K (#2708) were obtained from Cell Signaling Technologies. A monoclonal antibody for tubulin (#T5168) and horseradish peroxidase-conjugated goat anti-rabbit (#A0545) and goat anti-mouse secondary antibodies (#A9044) were obtained from Millipore Sigma.

Alkaline comet assay

The alkaline comet assay was carried out on cells 8 and 24 h after treatment with 11 and 16.5 nM of RAPA, or the volume equivalent of DMSO, combined with 3 or 6 Gy of radiation, following the protocols developed by Singh et al (22). The volume equivalents of DMSO for 11 nM and 16.5 nM of RAPA were designated as low and high concentrations, respectively. Slides were placed in chilled comet electrophoresis buffer for 30 min. The slides were electrophoresed for 40 min at 1 volt/cm.

After electrophoresis, the slides were washed with deionized water, then dehydrated with 100% ethanol, and air-dried. Slides were incubated in the dark with 30 μM 4′,6-diamidino-2-phenylindole (DAPI) diluted in a 1:100 ratio with PBS to fully cover the slide. Images were taken with a 20× objective lens using a Leica fluorescent microscope.

Cells were visually inspected and manually categorized into 1 of 4 categories based on the appearance of the amount of damage sustained (none, low, moderate, and extensive). Based on a previous study by Olive et al (23), cells with the appearance of a distinct, paddle-shaped tail were apoptotic and categorized as having 'extensive damage.' At least 100 cells were scored for each treatment, totaling over 300 cells/condition over 3 biological replicates.

Statistical analysis

Dunnett's multiple comparisons test determined differences in means for the clonogenic assay and in densitometry means for all western blots. Phosphorylated S6K band density was normalized to the native S6K band. This value was then normalized to the density of the tubulin band. Dunnett's multiple comparisons test was also used with comet assay data comparing radiation only *versus* DMSO. The Mann-Whitney test compared RAPA treatment with its DMSO equivalent vehicle control in the comet assay. Results were considered statistically significant when the *P*-value was ≤ 0.05.

Results

Clonogenic survival

Pre-treatment of MCT-1 cells with RAPA did not influence clonogenic survival at any dose of radiation, regardless of dose or incubation. MCT-1 clonogenic survival decreased as the IR dose increased. Observations are illustrated in Figure 1.

mTOR signaling

Western blots quantified relative levels of phosphorylated S6K as an indicator of changes in mTOR activity caused by RAPA, RT, or a combination of the two. As shown in Figure 2 A, C, 15 min of exposure to RAPA alone did not appear to significantly impact S6K phosphorylation in MCT-1 cells, but a dose-dependent response to

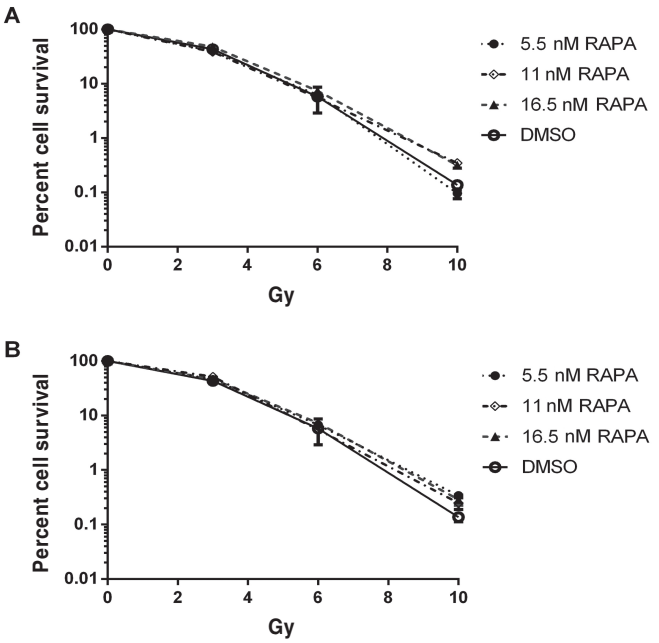

Figure 1. MCT-1 clonogenic survival relative to DMSO (means with SEM, *n* = 4). A — 24 h of pre-treatment with rapamycin (RAPA) combined with radiation. B — 48 h of pre-treatment with RAPA combined with radiation. Error bars represent SEM.

RAPA was observed after 30 min. Between 1 and 24 h, all doses of RAPA reduced S6K phosphorylation to undetectable levels in MCT-1 cells. Dimethyl sulfoxide alone increased S6K phosphorylation relative to control until at least 4 h in MCT-1 cells, but this DMSO affect was abrogated by 24 h. These patterns of S6K phosphorylation occurred more swiftly in MCT-2 cells, in which phosphorylation was reduced to undetectable levels at 15 min of exposure with all doses of RAPA and was sustained for up to 24 h (Figure 2 B, D).

Radiation therapy (RT) alone qualitatively increased S6K phosphorylation in MCT-1 cells up to 4 h after exposure to 6 and 10 Gy and up to 2 h after exposure to 3 Gy (Figure 3 A, C), although these differences were not statistically significant. In MCT-2 cells, 10 Gy of RT alone also increased mTOR activity, which was statistically significant for all timepoints except for 8 h (Figure 3 B, D).

The combination of RT and RAPA resulted in the inhibition of mTOR signaling in both MCT-1 and MCT-2 cells. After 30 min of exposure to 10 Gy, in combination with every dose of RAPA, S6K phosphorylation was completely undetectable in MCT-1 cell lysates (Figure 4 A, C). In MCT-2 cells, S6K phosphorylation was affected in an almost identical manner (Figure 4 B, D). This trend continued with all other timepoints up to 24 h; timepoints up to 2 h are shown in Figure 4.

The blots and densitometry for all other time points and for RAPA combined with 3 and 6 Gy of IR are shown in the supplementary figures (Figures S1 to S5) available online at https://hdl.handle.net/10214/26557. The trends observed in the RAPA and 10 Gy combination were also observed with 3 and 6 Gy.

DNA damage

The comet assay quantified the extent of DNA damage sustained on an individual cell basis. Examples of images of the comet assay from control cells and cells treated with 3 or 6 Gy are shown in

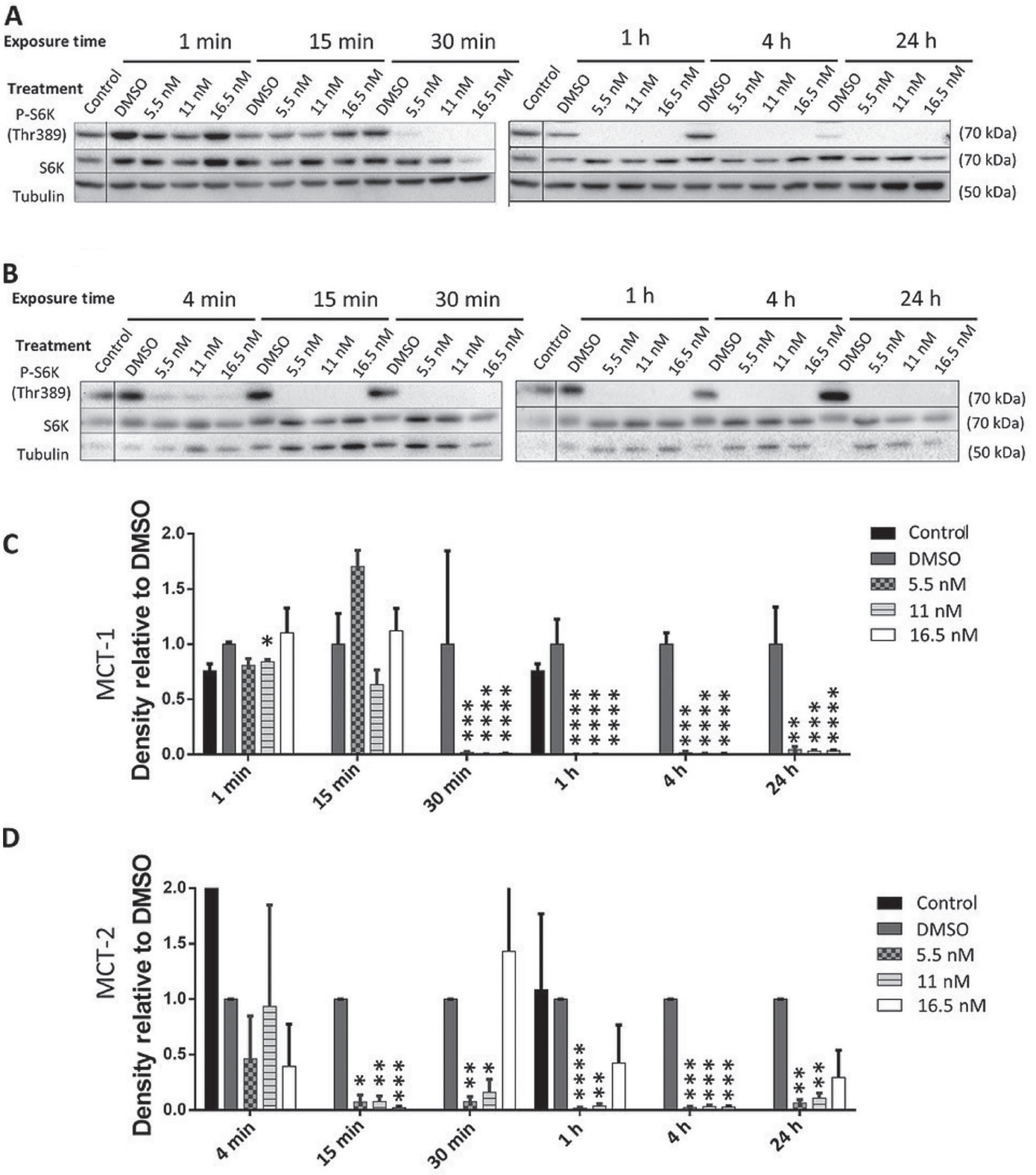

Figure 2. Western blots of phosphorylated S6K (Thr389) in MCT-1 (A) and MCT-2 (B) lysates after exposure to rapamycin (RAPA). For the densitometry analysis of MCT-1 (C) and MCT-2 (D), the ratio of p-S6K:native S6K:tubulin was calculated for each treatment and normalized to the DMSO control for that time point.

***n* = 3 (**P* ≤ 0.05, ***P* ≤ 0.01, ****P* ≤ 0.001, *****P* ≤ 0.0001). Error bars represent SEM.**

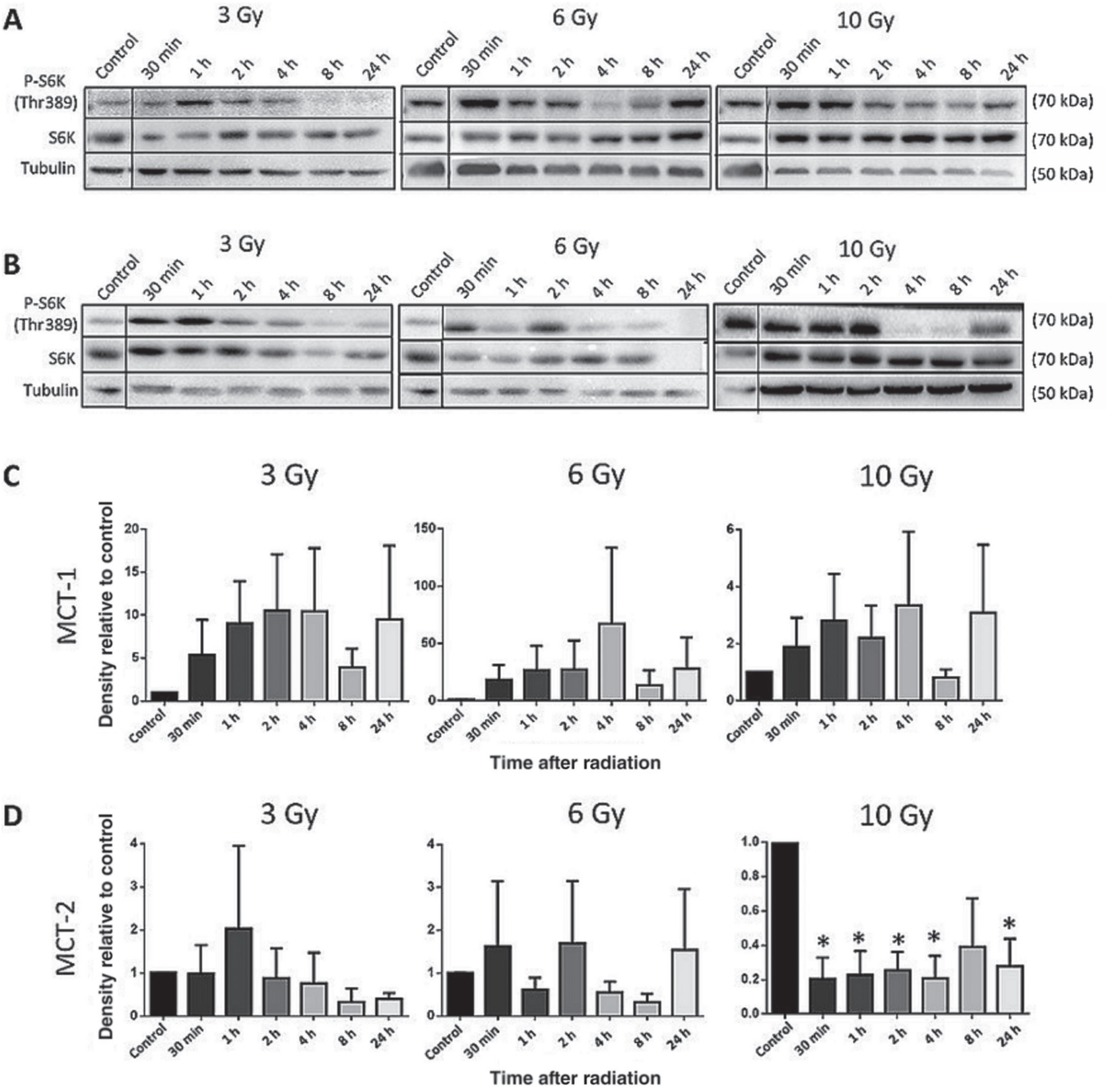

Figure 3. Western blots of phosphorylated S6K (Thr389) in MCT-1 (A) and MCT-2 (B) lysates 30 min to 24 h after exposure to 3, 6, or 10 Gy. For the densitometry analysis of MCT-1 (C) and MCT-2 (D), the ratio of p-S6K:native S6K:tubulin was calculated for each treatment and normalized to the DMSO control for that time point.

***n* = 3 (**P* ≤ 0.05). Error bars represent SEM.**

Figure 5 A to C. Data in Figure 5 D to G suggest that DMSO reduced the percentage of MCT cells with extensive DNA damage when treated with either 3 or 6 Gy of RT. The percentage of MCT-1 cells with extensive DNA damage when treated with a combination of 3 Gy and RAPA was inconsistent, whereas MCT-2 tended to have a higher percentage of damaged cells in RAPA groups compared to their DMSO groups.

In both cell lines, treatment with 6 Gy combined with either dose of RAPA was more effective at causing extensive DNA damage than the equivalent DMSO concentration or RT only (Figure 5 E, G). The only exception to this was the 24-hour incubation period with MCT-2 cells. In this case, 16.5 nM of RAPA generated more severely damaged cells than the equivalent concentration of DMSO, but not more than RT only (Figure 5 G). Although these trends suggest that RAPA

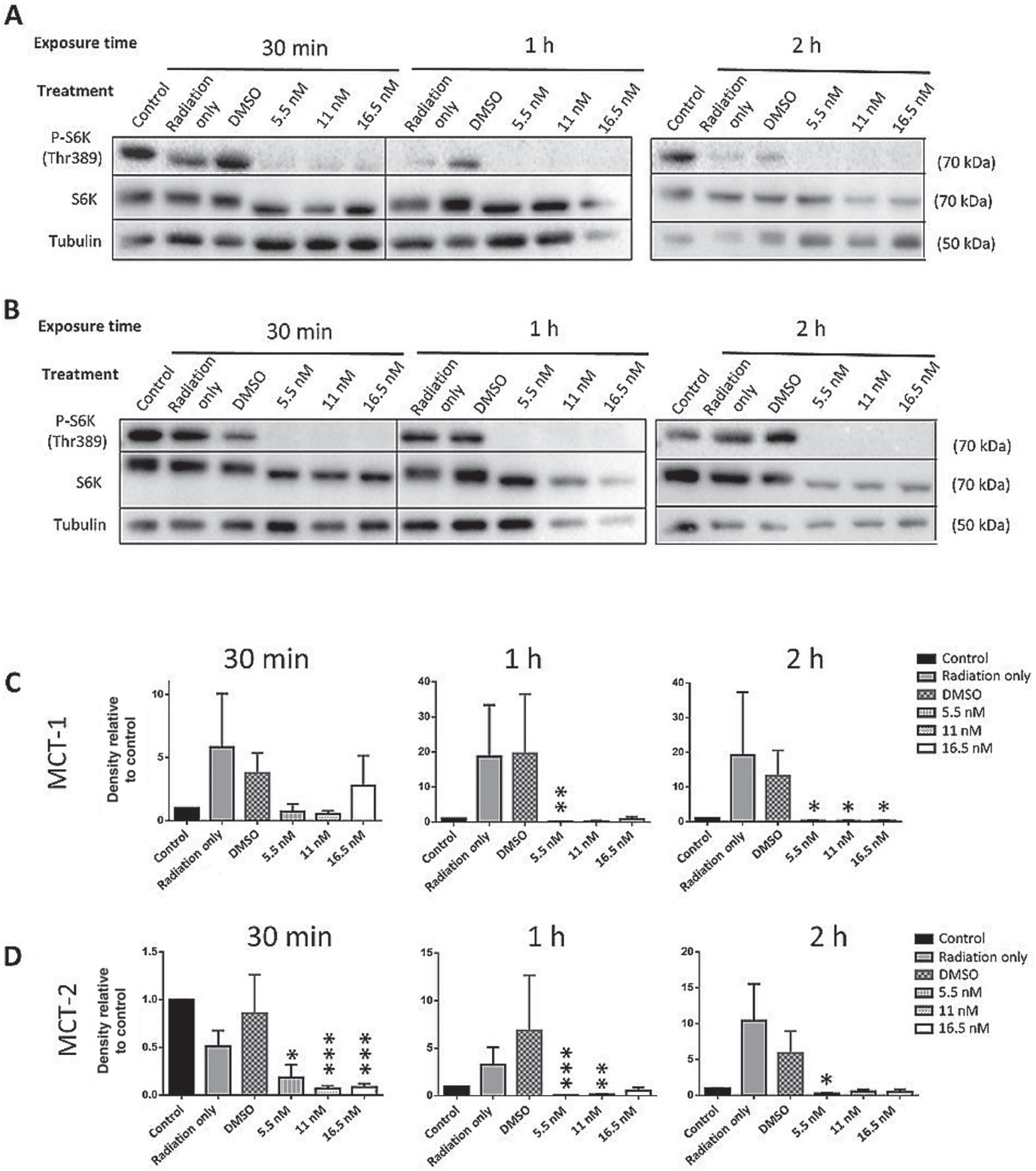

Figure 4. Western blots of phosphorylated S6K (Thr389) in MCT-1 (A) and MCT-2 (B) lysates 30 min to 2 h after treatment with 10 Gy of radiation therapy and rapamycin (RAPA). For the densitometry analysis of MCT-1 (C) and MCT-2 (D), the ratio of p-S6K:native S6K:tubulin was calculated for each treatment and normalized to the DMSO control for that time point.

***n* = 3 (**P* ≤ 0.05, ***P* ≤ 0.01, ****P* ≤ 0.001). Error bars represent SEM.**

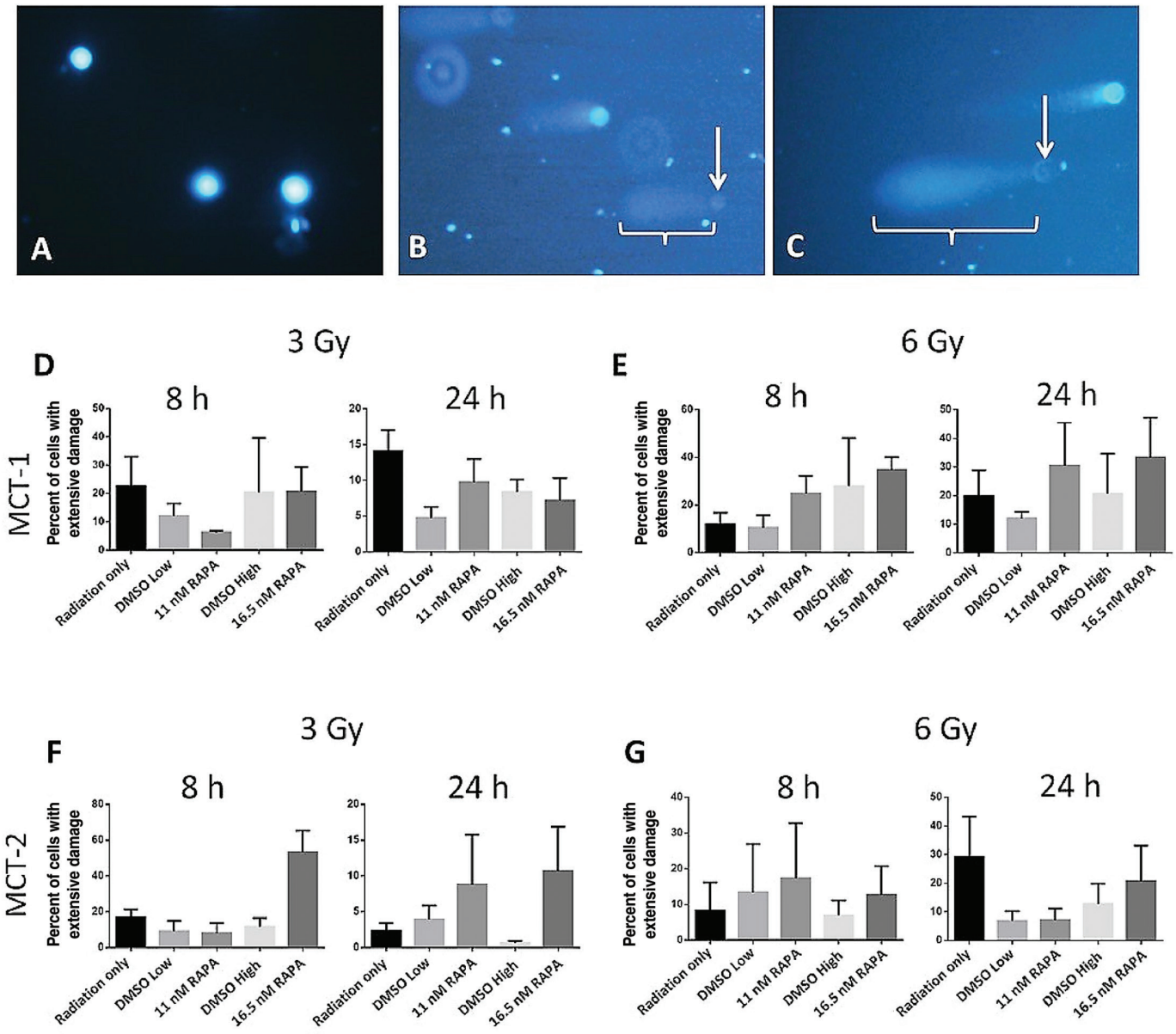

Figure 5. Examples of the comet assay results with MCT-1 cells stained with DAPI after treatment with no radiation (A), 3 Gy and High DMSO (B), and 6 Gy and 11 nM of rapamycin (RAPA) (C). The white arrows indicate cells designated as having extensively damaged DNA, showing a faint nucleus and paddle-shaped tail (brackets). Graphs show the percentage of MCT-1 cells that sustained extensive DNA damage 8 h and 24 h after exposure to 3 Gy (D) and 6 Gy (E) combined with RAPA and the percentage of MCT-2 cells that sustained extensive DNA damage 8 h and 24 h after exposure to 3 Gy (F) and 6 Gy (G) combined with RAPA.

***n* = 3. Error bars represent SEM.**

may have a radiosensitizing effect, none of the observations in the comet assay were found to be statistically significant.

Discussion

mTOR hyperactivation is observed in many cancers, aiding in both avoiding oncogenic restraint and promoting growth or metastasis. Constitutive activation leads to increased 4E-BP1, enhancing pro-oncogenic protein synthesis, as well as contributing to the Warburg effect by promoting activation of transcription factors like hypoxia-inducible factor 1α (24,25). mTOR dysregulation also contributes to escaping autophagy by disrupting critical components to autophagy initiation, such as UNC-5-like autophagy-activating kinase complex or autophagy-initiating kinases (26,27).

Although the mTOR pathway is traditionally associated with several essential cell survival functions, it is not commonly associated with DNA damage response (DDR). Several studies have suggested that, in some scenarios, the effectiveness of cancer therapies that target DNA can be enhanced by inhibiting the mTOR pathway (11,28,29). The growth of doxorubicin-resistant human prostate cancer xenografts was inhibited when doxorubicin was combined with a RAPA derivative (30). Cell proliferation of human non-small

cell lung cancer and triple negative breast cancer was synergistically inhibited when the poly (adenosine diphosphate-ribose) polymerase (PARP) inhibitor olaparib and RAPA were used concurrently (31).

It has also been observed that RAPA increases the effectiveness of radiation therapy (RT) at inducing apoptosis in human non-small cell lung cancer (32). Combining RAPA with chemotherapy, non-chemotherapeutic medication, or RT, all of which have different mechanisms of action, was beneficial in these scenarios. The commonality these regimens share is their interaction with DNA damage responses (DDRs). Inhibiting mTOR signaling may simply turn off pro-survival signals, but the results of the previously mentioned studies allude to a more specific consequence.

We expected that our canine mast cell cancer cells would respond to RAPA and RT combination therapy in a similar manner. For cells treated with RT only, there was an apparent dose-dependent stimulatory response in mTOR signaling, which suggests interaction with the DNA damage response. Although Nagata et al (32) observed in non-small cell lung cancer that RT increased phosphorylation levels of Akt and mTOR, components upstream of S6K, and S6, the downstream target of S6K, their study did not look at phosphorylation levels of S6K itself. It is thus unclear if the potential increase in phosphorylation of S6K observed in our study was caused by RT directly or was a result of upstream activation. Regardless, it suggests that a cell's response to DNA damage manifests in the activation of the mTOR signaling cascade.

In our study, treatment with RAPA alone was able to strongly, if not completely, inhibit mTOR signaling in both MCT-1 and MCT-2 cells after 30 and 15 min, respectively. The same response was observed for the combination of RT and RAPA. Given such robust inhibition of signaling, we hypothesized that any effect mTOR might have had on the cells' subsequent response to RT-induced DNA damage was effectively inhibited.

The comet assay was used to visualize and quantify the DNA damage (in the form of strand breaks) sustained by both cell lines following treatment with a combination of RAPA and RT. Two vehicle controls, DMSO volume equivalents of the 2 RAPA concentrations, were assessed in this assay to control for any effects that DMSO alone might have on DNA damage response (DDR). Free radicals form when water absorbs ionizing radiation, generating entities such as hydroxyls that can cause multiple forms of DNA damage, including strand breaks (33).

In MCF-7 cells, DMSO is known to be a free-radical scavenger at concentrations as low as 1 mM (34). The highest DMSO concentration in our experiments was 23.3 mM, but DMSO did not appear to make a significant or consistent difference in protecting cells from extensive DNA damage. Although some studies suggest that DMSO does not affect mTOR signaling (35,36), our MCT-1 cells treated with RAPA alone showed a trend that DMSO may have increased mTOR signaling. The ability of DMSO to reduce the percentage of extensively damaged irradiated cells compared to cells that received only RT was generally stronger in MCT-2 than in MCT-1 cells. There was also a general trend across both irradiated cell lines for RAPA to increase the percentage of extensively damaged cells compared to its DMSO equivalent for both incubation periods. Although none of the comet assay results was found to be statistically significant after 3 biological replicates, there was an arguable consistency indicating that RAPA-treated groups differed in response to their DMSO and RT-only controls.

The lack of statistical significance in the comet assay fails to provide evidence that RAPA influences the amount of DNA damage sustained from RT. It has been observed that mTOR negatively regulates protein phosphatase 2A (PP2A), an enzyme believed to dephosphorylate the histone subunit H2AX, whereas RAPA increases PP2A activity (37). Phosphorylated H2AX is a marker for sites of DNA damage. PP2A also activates DNA-PK, a necessary component of non-homologous end joining (38). This suggests that RAPA could have a protective effect on DNA damage, which conflicts with the previously mentioned studies that report the opposite. More importantly, it suggests that the mTOR pathway does play a role in regulating DDR.

The clonogenic survival assays demonstrated that, regardless of RAPA pre-treatment, 6 Gy of RT killed over 92% of MCT-1 cells, which suggests that this cell line is highly radio-sensitive in comparison to H1299, a lung cancer cell line that was observed to experience approximately 80% of clonogenic cell death at 8 Gy (39). Despite extreme mTOR inhibition up to the clinically high single dose of 10 Gy, any possible synergistic effects brought on by RAPA may have been overshadowed by an already present inability to repair DNA damage by the MCT-1 cells. Therefore, it would be worthwhile to repeat these experiments in radio-resistant canine mast cell cancer cell lines to observe whether RAPA can restore sensitivity.

The previously referenced studies used similar RAPA concentrations (ranging from 1 to 10 nM) to achieve enhanced cancer growth inhibition or apoptosis. The lung cancer study by Nagata et al (32), however, used a higher concentration of RAPA (100 nM) on their H1299 cell line. Similarly, a study using MCF7 cells observed that combining RT with 27.3 nM of RAPA impaired double strand break (DSB) repair using the comet assay (13). Increased RAPA concentrations could lead to off-target effects, which could explain why these studies observed more changes in cell survival and DNA damage after similar RT exposure.

The effects of mTOR inhibition on DNA damage response (DDR) could vary depending on upstream factors. For example, active phosphatase and tensin homolog (PTEN) inhibits Akt activity, resulting in a decrease in mTOR activation (40). Therefore, RAPA could have a synergistic effect in cells with an active PTEN status but have an increased threshold to be effective in cells with a PTEN mutation or deficiency. Canine mast cell tumors with a detected loss of PTEN function have been reported to have worse prognoses (41). Loss of PTEN function has also been observed in some canine osteosarcoma, melanoma, hemangiosarcoma, and prostate cancers (42–45), which suggests that aberrations in this gene are common in canine malignancies. The status of such relevant genes could be an important consideration in both a tumor's pathogenesis and response to therapy.

In conclusion, RAPA is an effective and accessible reagent to inhibit mTOR signaling. Although the exact relationship between this pathway and the DNA damage response induced by RT has yet to be elucidated, our study suggests some interaction between the 2 processes. There are clinical benefits to developing a method to increase the efficacy of RT without needing to increase the dose or combine it with cytotoxic chemotherapy. The action of RAPA as a

radiosensitizer appears highly variable, however, and may depend on the type of cancer. The clinical usefulness of RAPA in canine mast cell cancer is therefore unclear.

Acknowledgments

This project was supported by the Ontario Veterinary College Pet Trust. Morla Phan was awarded an Art Rouse Cancer Biology Scholarship to assist with her work on this project. Thanks to Jennifer Thompson for providing the MCT-1 and MCT-2 cell lines, Laura Furness for irradiating the cells, and Jodi Morrison for general technical support.

References

1. Ilyinskaya GV, Mukhina EV, Soboleva AV, Matveeva OV, Chumakov PM. Oncolytic sendai virus therapy of canine mast cell tumors (a pilot study). Front Vet Sci 2018;5:116.
2. Zemke D, Yamini B, Yuzbasiyan-Gurkan V. Mutations in the juxtamembrane domain of c-KIT are associated with higher grade mast cell tumors in dogs. Vet Pathol 2002;39:529–535.
3. Letard S, Yang Y, Hanssens K, et al. Gain-of-function mutations in the extracellular domain of KIT are common in canine mast cell tumors. Mol Cancer Res 2008;6:1137–1145.
4. London CA, Galli SJ, Yuuki T, Hu ZQ, Helfand SC, Geissler EN. Spontaneous canine mast cell tumors express tandem duplications in the proto-oncogene c-kit. Exp Hematol 1999;27:689–697.
5. Hahn KA, King GK, Carreras JK. Efficacy of radiation therapy for incompletely resected grade-III mast cell tumors in dogs: 31 cases (1987–1998). J Am Vet Med Assoc 2004;224:79–82.
6. London CA, Malpas PB, Wood-Follis SL, et al. Multi-center, placebo-controlled, double-blind, randomized study of oral toceranib phosphate (SU11654), a receptor tyrosine kinase inhibitor, for the treatment of dogs with recurrent (either local or distant) mast cell tumor following surgical excision. Clin Cancer Res 2009;15:3856–3865.
7. Sharma V, Sanghavi V, Agarwal JP, et al. Single institution prospective randomized trial of radiation as a sole modality in palliation of advanced non-small cell lung cancer — An international atomic energy agency study. Sci Rep 2012;1:1–8.
8. Minsky BD. Palliation of esophageal cancer: Palliative external beam radiation therapy and combined modality therapy. Dis Esophagus 1996;9:86–89.
9. Fu S, Li Z, Xiao L, et al. Glutamine synthetase promotes radiation resistance via facilitating nucleotide metabolism and subsequent DNA damage repair. Cell Rep 2019;28:1136–1143.
10. Kratochwil C, Giesel FL, Heussel CP, et al. Patients resistant against PSMA-targeting α-radiation therapy often harbor mutations in DNA damage-repair-associated genes. J Nucl Med 2020; 61:683–688.
11. Li Y, Liu F, Wang Y, et al. Rapamycin-induced autophagy sensitizes A549 cells to radiation associated with DNA damage repair inhibition. Thorac Cancer 2016;7:379–386.
12. Assad DX, Borges GA, Avelino SR, Guerra ENS. Additive cytotoxic effects of radiation and mTOR inhibitors in a cervical cancer cell line. Pathol Res Pract 2018;214:259–262.
13. Chen H, Ma Z, Vanderwaal RP, et al. The mTOR inhibitor rapamycin suppresses DNA double-strand break repair. Radiat Res 2011;175:214–224.
14. Laplante M, Sabatini DM. mTOR signaling in growth control and disease. Cell 2012;149:274–293.
15. Feng Z, Zhang H, Levine AJ, Jin S. The coordinate regulation of the p53 and mTOR pathways in cells. Proc Natl Acad Sci U S A 2005;102:8204–8209.
16. Thompson JJ. Canine mast cell tumours: Characterization of subcutaneous tumours and receptor tyrosine kinase profiling. [PhD dissertation]. Guelph, Ontario: University of Guelph, 2012.
17. Larson JC, Allstadt SD, Fan TM, et al. Pharmacokinetics of orally administered low-dose rapamycin in healthy dogs. Am J Vet Res 2016;77:65–71.
18. Poirier VJ, Adams WM, Forrest LF, Green EM, Dubielzig RR, Vail DM. Radiation therapy for incompletely excised grade II canine mast cell tumors. J Am Anim Hosp Assoc 2006;42:430–434.
19. Carlsten KS, London CA, Haney S, Burnett R, Avery AC, Thamm DH. Multicenter prospective trial of hypofractionated radiation treatment, toceranib, and prednisone for measurable canine mast cell tumors. J Vet Intern Med 2012;26:135–141.
20. Gieger TL, Nolan MW. Linac-based stereotactic radiation therapy for canine non-lymphomatous nasal tumours: 29 cases (2013–2016). Vet Comp Oncol 2018;16:E68–E75.
21. Mantovani FB, Morrison JA, Mutsaers AJ. Effects of epidermal growth factor receptor kinase inhibition on radiation response in canine osteosarcoma cells. BMC Vet Res 2016;12:82.
22. Singh NP, McCoy MT, Tice RR, Schneider EL. A simple technique for quantitation of low levels of DNA damage in individual cells. Exp Cell Res 1988;175:184–191.
23. Olive PL, Frazer G, Banáth JP. Radiation-induced apoptosis measured in TK6 human B lymphoblast cells using the comet assay. Radiat Res 1993;136:130–136.
24. Gingras AC, Kennedy SG, O'Leary MA, Sonenberg N, Hay N. 4E-BP1, a repressor of mRNA translation, is phosphorylated and inactivated by the Akt(PKB) signaling pathway. Genes Dev 1998;12:502–513.
25. Shen Y, Liu Y, Sun T, Yang W. LincRNA-p21 knockdown enhances radiosensitivity of hypoxic tumor cells by reducing autophagy through HIF-1/Akt/mTOR/P70S6K pathway. Exp Cell Res 2017;358:188–198.
26. Ganley IG, Lam du H, Wang J, Ding X, Chen S, Jiang X. ULK1. ATG13.FIP200 complex mediates mTOR signaling and is essential for autophagy. J Biol Chem 2009;284:12297–12305.
27. Kamada Y, Funakoshi T, Shintani T, Nagano K, Ohsumi M, Ohsumi Y. Tor-mediated induction of autophagy via an Apg1 protein kinase complex. J Cell Biol 2000;150:1507–1513.
28. Mondesire WH, Jian W, Zhang H, et al. Targeting mammalian target of rapamycin synergistically enhances chemotherapy-induced cytotoxicity in breast cancer cells. Clin Cancer Res 2004;10:7031–7042.
29. Eshleman JS, Carlson BL, Mladek AC, Kastner BD, Shide KL, Sarkaria JN. Inhibition of the mammalian target of rapamycin sensitizes U87 xenografts to fractionated radiation therapy. Cancer Res 2002;62:7291–7297.

30. Grünwald V, DeGraffenried L, Russel D, Friedrichs WE, Ray RB, Hidalgo M. Inhibitors of mTOR reverse doxorubicin resistance conferred by PTEN status in prostate cancer cells. Cancer Res 2002;62:6141–6145.
31. Osoegawa A, Gills JJ, Kawabata S, Dennis PA. Rapamycin sensitizes cancer cells to growth inhibition by the PARP inhibitor olaparib. Oncotarget 2017;8:87044–87053.
32. Nagata Y, Takahashi A, Ohnishi K, et al. Effect of rapamycin, an mTOR inhibitor, on radiation sensitivity of lung cancer cells having different p53 gene status. Int J Oncol 2010;37:1001–1010.
33. Smith TA, Kirkpatrick DR, Smith S, et al. Radioprotective agents to prevent cellular damage due to ionizing radiation. J Transl Med 2017;15:232.
34. Yang C, Tang H, Wang L, et al. Dimethyl sulfoxide prevents radiation-induced oral mucositis through facilitating DNA double-strand break repair in epithelial stem cells. Int J Radiat Oncol Biol Phys 2018;102:1577–1589.
35. Yellen P, Saqcena M, Salloum D, et al. High-dose rapamycin induces apoptosis in human cancer cells by dissociating mTOR complex 1 and suppressing phosphorylation of 4E-BP1. Cell Cycle 2011;10:3948–3956.
36. Song YM, Song SO, Jung YK, et al. Dimethyl sulfoxide reduces hepatocellular lipid accumulation through autophagy induction. Autophagy 2012;8:1085–1097.
37. Li Y, Wang X, Yue D, et al. Protein phosphatase 2A and DNA-dependent protein kinase are involved in mediating rapamycin-induced Akt phosphorylation. J Biol Chem 2013;288: 13215–13224.
38. Douglas P, Moorhead GB, Ye R, Lees-Miller SP. Protein phosphatases regulate DNA-dependent protein kinase activity. J Biol Chem 2001;276:18992–18998.
39. Balça-Silva J, Neves SS, Gonçalves AC, et al. Effect of miR-34b overexpression on the radiosensitivity of non-small cell lung cancer cell lines. Anticancer Res 2012;32:1603–1609.
40. Ortega-Molina A, Serrano M. PTEN in cancer, metabolism, and aging. Trends Endocrinol Metab 2013;24:184–189.
41. Jark PC, Mundin DPB, de Carvalho M, et al. Genomic copy number variation associated with clinical outcome in canine cutaneous mast cell tumors. Res Vet Sci 2017;111:26–30.
42. Levine RA, Forest T, Smith C. Tumor suppressor PTEN is mutated in canine osteosarcoma cell lines and tumors. Vet Pathol 2002;39:372–378.
43. Rivera-Calderón LG, Fonseca-Alves CE, Kobayashi PE, et al. Alterations in PTEN, MDM2, TP53 and AR protein and gene expression are associated with canine prostate carcinogenesis. Res Vet Sci 2016;106:56–61.
44. Koenig A, Bianco SR, Fosmire S, Wojcieszyn J, Modiano JF. Expression and significance of p53, rb, p21/waf-1, p16/ink-4a, and PTEN tumor suppressors in canine melanoma. Vet Pathol 2002;39:458–472.
45. Dickerson EB, Thomas R, Fosmire SP, et al. Mutations of phosphatase and tensin homolog deleted from chromosome 10 in canine hemangiosarcoma. Vet Pathol 2005;42:618–632.